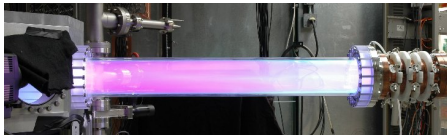


Plasma Jet Research at HyperV Technologies*

F. Douglas Witherspoon, Andrew Case,
Sarah J. Messer, Richard Bomgardner, Sam Brockington

LANL Plasma Jet Workshop
January 24-25, 2008
Los Alamos, NM

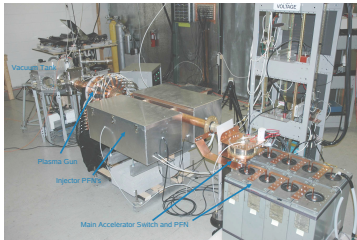


*Work funded by the U.S. DOE Office of Fusion Energy Sciences

Background

Applications

- Magneto-Inertial Fusion
- Magnetic Confinement Devices
- High Energy Density Laboratory Plasmas
- Simulating Astrophysical Jets
- Plasma Thrusters
- Materials Processing



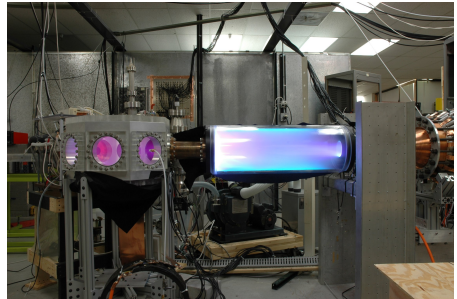
Technical Goals

velocity $> 200 \text{ km/s}$

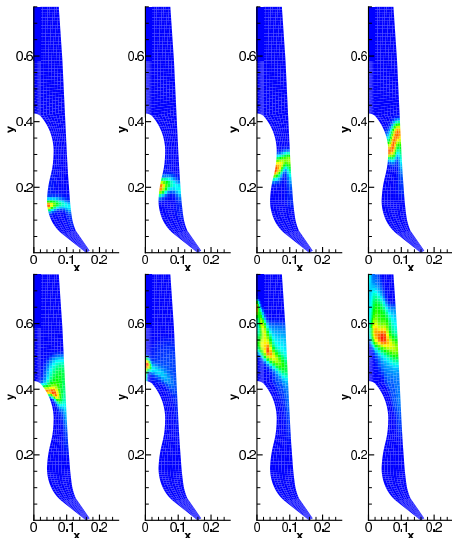
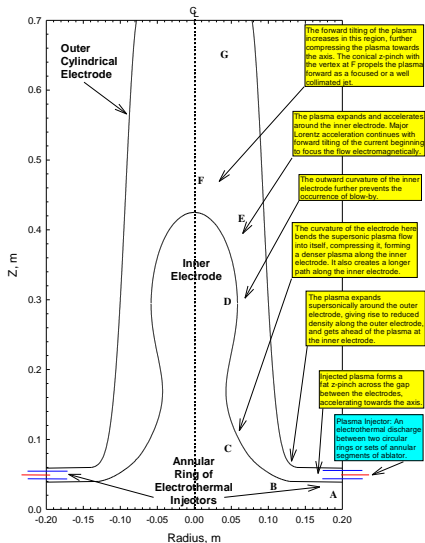
mass $\simeq 100 - 200 \mu\text{g}$

density $\simeq 10^{16} - 10^{17} \text{ cm}^{-3}$

Mach $\simeq 10 - 20$



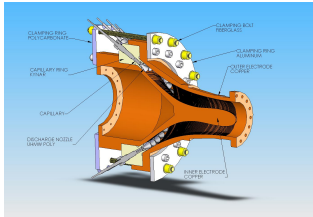
Electrode Profile Tailoring Can Suppress Blow-By Instability by Matching Density with $J \times B$



Four Main Experimental Efforts at Present

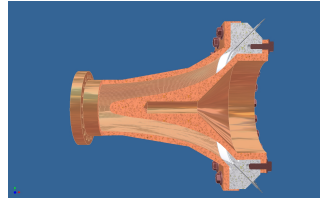
Wasp Profile

32 ablative capillary injectors, now on MCX



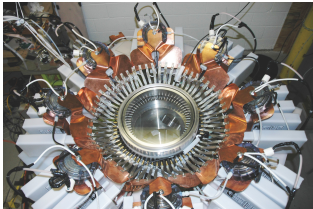
Circular Arc Profile

112 sparkgap tips



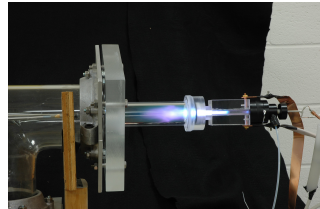
TwoPi

64 ablative capillary injectors



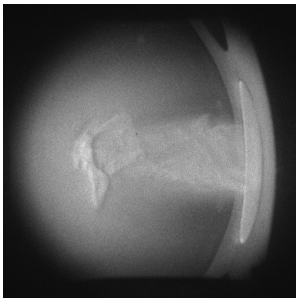
MiniRailgun Injector

Non-ablative pure gas injection

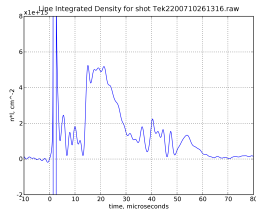


Side Views Show Jet Structure

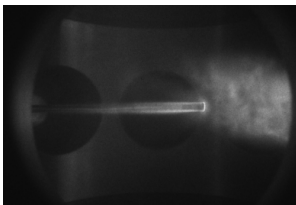
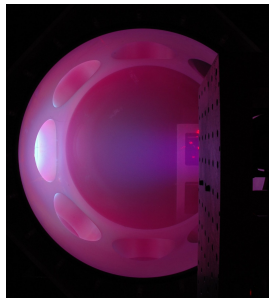
PImax image
25 ns gate



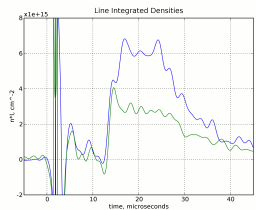
Interferometer data



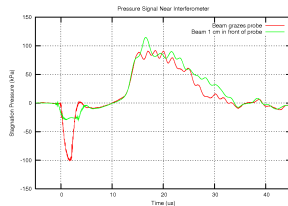
Nikon D70s image
2 sec exposure



Jet front impacts probe



Line integrated density

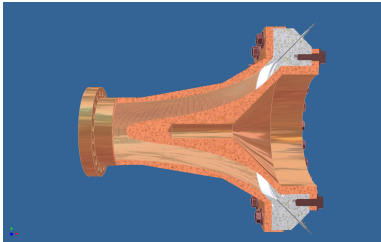


Pressure pulse coincides with line integrated density at left.

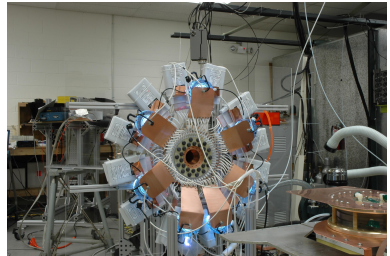
Sparkgap Approach Provides Better Injection Symmetry

More Energy Generates Increased Mass

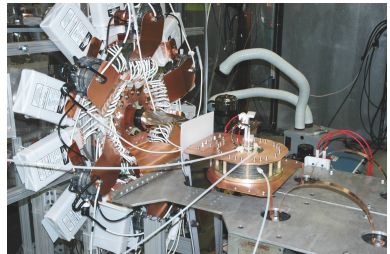
Circular Arc Profile vs. Wasp



Vacuum tested to mid- 10^{-6} Torr



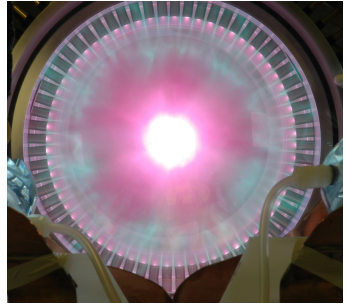
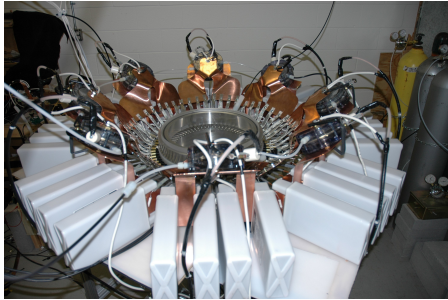
- 112 Tungsten electrodes provide “toroidal” capillaries
- Tips flush with polyethylene ablator surface
- Alternating polarity
- Provides “toroidal” capillaries
- Test circular arc profile
- Higher energy input $\rightarrow 360 \mu\text{g}$



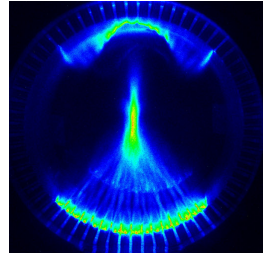
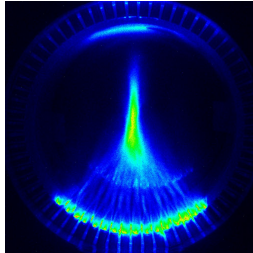
Plasma Jet Results to Date

- Momentum/Mass
 - 13 g-m/s (ballistic pendulum)
 - 160 μg at 85 km/s
- Density
 - *mid* – 10^{15} cm^{-3} (Stark broadening, before recent gun mods)
 - *mid* – 10^{14} cm^{-3} (interfer., Stark Broadening after recent gun mods)
- Velocity
 - Bulk, $\sim 75 - 90$ km/s (Doppler, photodiodes, fast imaging)
 - Fast component H up to 145 km/s (Doppler, photodiodes, imaging)
 - Fast component C up to 110 km/s (Doppler, photodiodes, imaging)
- Temperature
 - 4 eV (spectroscopy)
- Stagnation Pressure
 - 90 kPa (piezoelectric transducer)
- Velocity is reduced by
 - Transverse B field
 - Long plastic tubes
 - Surrounding conducting loops
 - High base pressure

The Higher Energy TwoPi Injector Test Fixture

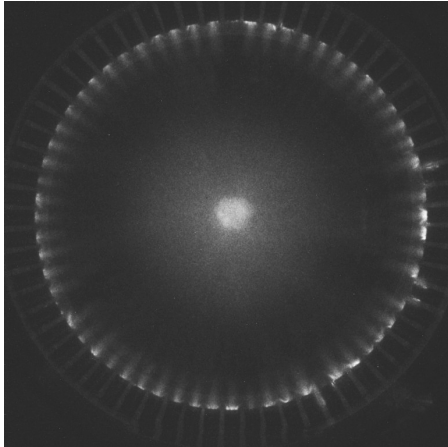


- Better vac - 10^{-5} Torr
- Better diagnostic access
- Smaller nozzle separation
- Tungsten electrodes
- More flexible
- Large vertical gap



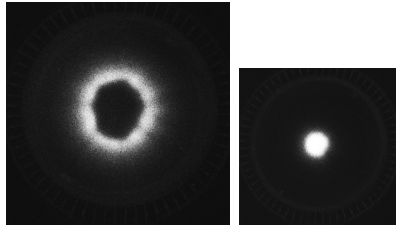
A Fast Symmetric Implosion on Upgraded TwoPi

Precursor implosion at $v \sim 80 \text{ km/s}$
25 ns PImax photo at $3.3 \mu\text{s}$



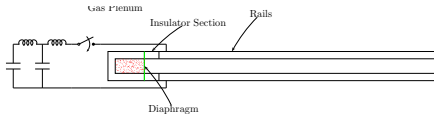
| | $n_e \text{ (cm}^{-3}\text{)}$ | $T_e \text{ (eV)}$ |
|-----------|--------------------------------|--------------------|
| periphery | 2.4×10^{14} | 2.4 |
| center | 2.5×10^{15} | 4.0 |

Main plasma shell follows later

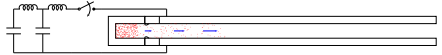


A MiniRailgun Can Provide a Pulsed High Mass Plasma Injector

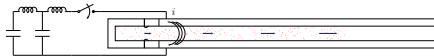
Initial Conditions
Pre-pressurized plenum, burst disk



Diaphragm Bursts
Energetic spark provides energy



Main Armature Forms
Gas/plasma fills bore



Armature Sweeps up Plasma
Delivers pulse at muzzle

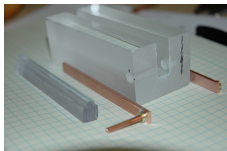


The pulse heated Plenum by itself may be sufficient!

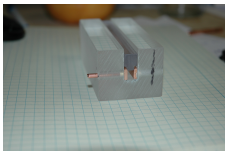
- nonablative ceramic
- tungsten sparkgap, tantalum diaphragm
- pulse heat stored gas

- short plenum
- very fast outflow $2\ell/c_s$
- only works if jitter is small

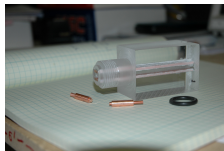
Stages of Assembly of 1st Gen MiniRailgun



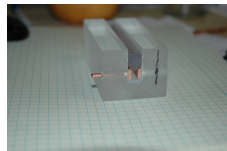
Initial copper rail busbar and acrylic insulator components.



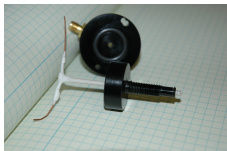
First step of assembly.



Side view showing brass current feeds and sealing nose O-ring.



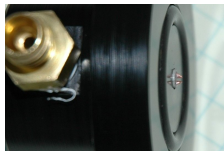
With one current feed in place.



Initial plenum components. White tee structure is the sparkgap electrode leads with insulation.



Closeup of the sparkgap tips barely protruding through surface of plenum back wall.

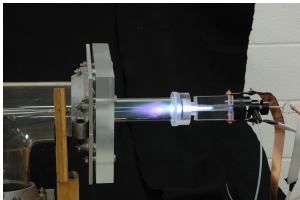


Side view of sparkgap tips.

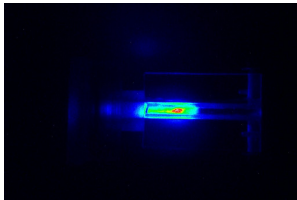


Side view of assembled unit.

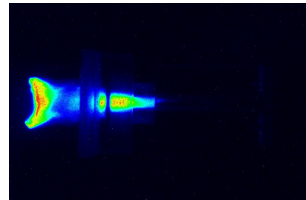
MiniRailgun Armature and Plume Imaging



A 1 sec exposure with Nikon D70s in the 10cm MiniRailgun.

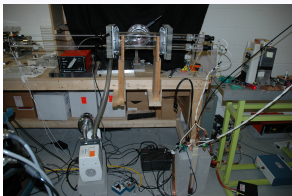


Fast PImax image of armature halfway down the bore. 25 ns gate width, $5\ \mu\text{s}$ after trigger.

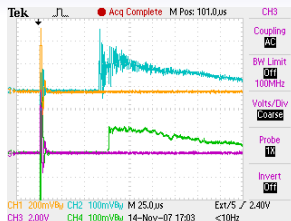


Fast PImax image of arc at end of rails and plasma jet plume extending into the vacuum chamber. 25 ns gate width, $20\ \mu\text{s}$ after trigger.

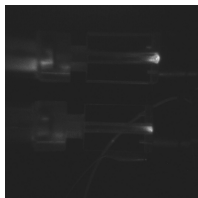
Dual MiniRailgun Tests Confirm Small Jitter



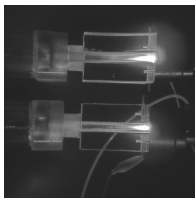
Experimental setup for dual railgun tests to investigate diaphragm burst jitter.



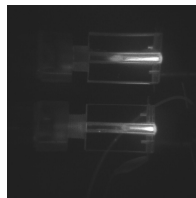
Signals on two separate pressure probes just downstream of the railgun muzzles. The base pressure here was about 1 Torr.



Light emission from the burst diaphragm appears within less than $1 \mu s$ from each plenum.



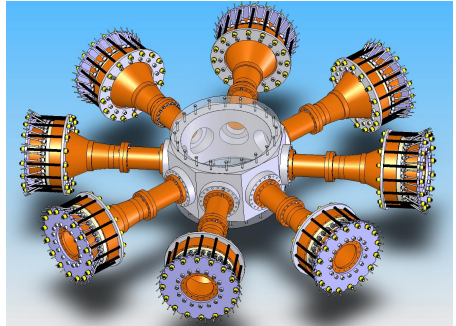
Fast Plmax image of armature halfway down the bore. 25 ns gate width, $5 \mu s$ after trigger.



A 25 ns gate at $10 \mu s$.

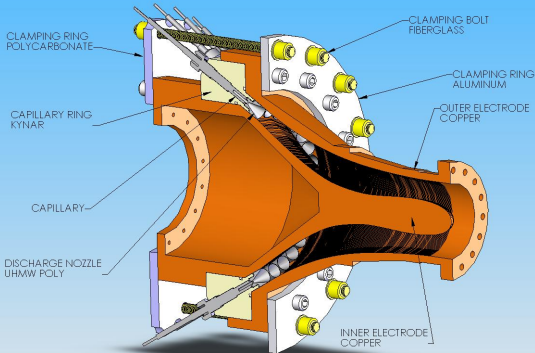
Summary

- Demonstrated Plasma Injection into Coaxial Plasma Gun
 - Ablative Capillaries
 - Good Jitter
 - Achieved $160\text{ }\mu\text{g}$ at 85 km/s
 - Needs more energy
- Suite of Diagnostics Developed
- Performed Initial Jet Merging Experiments
- Pulsed MiniRailgun Injector under Development

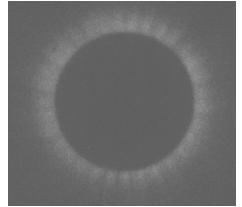


Backup Slides

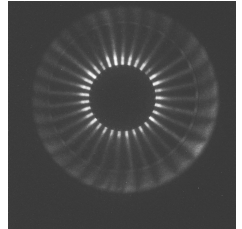
HyperV Plasma Jet Internal Structure



25 ns gate at $t = 0$

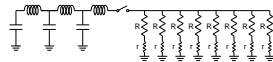


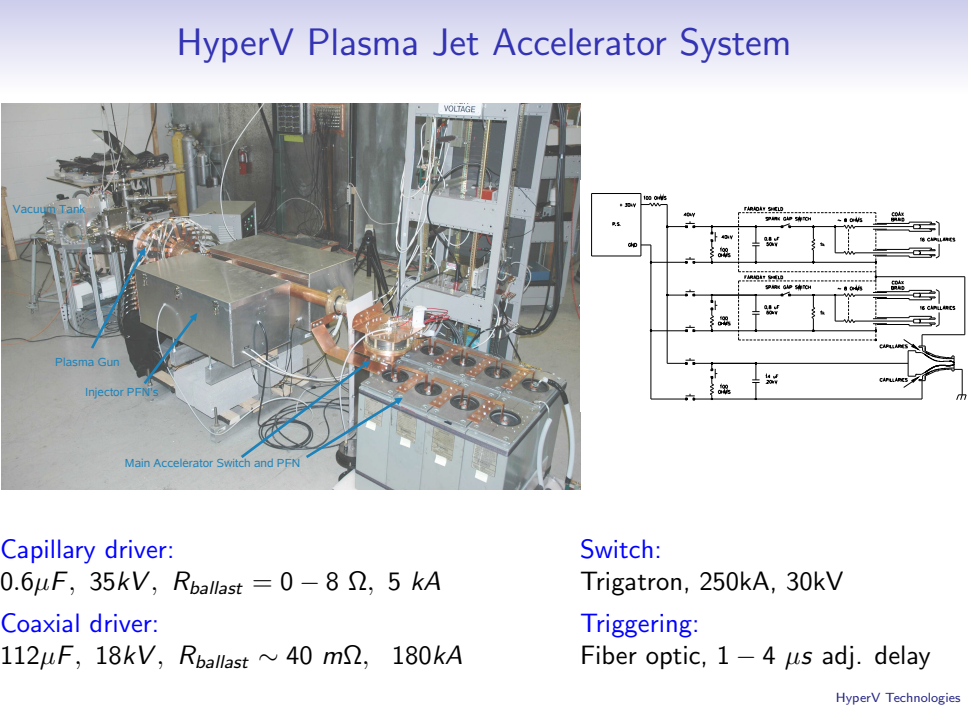
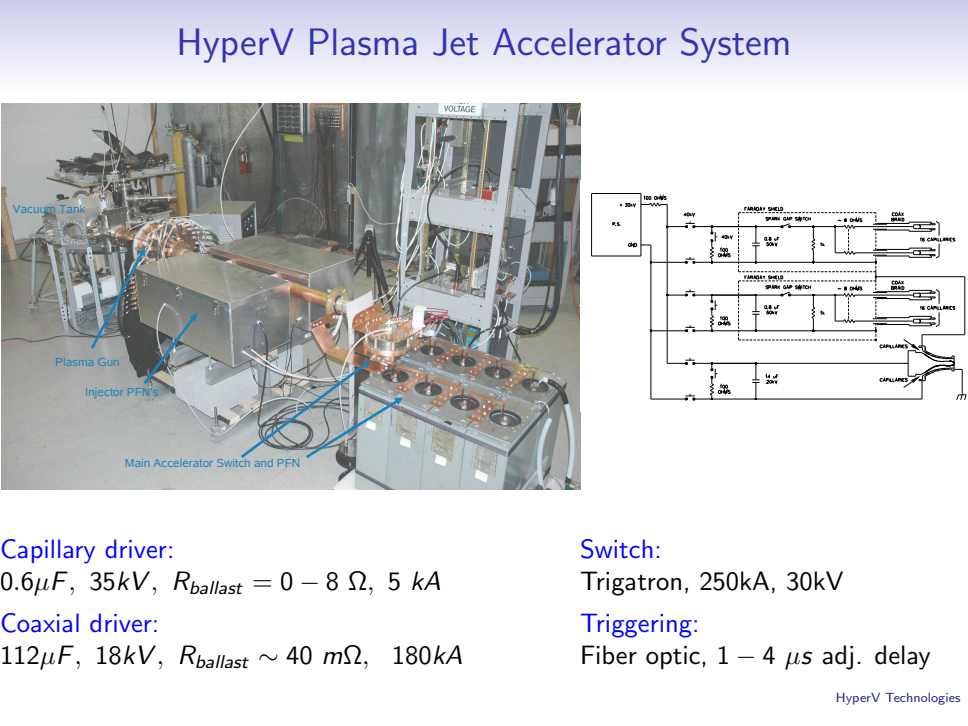
25 ns gate, $t = 1.3 \mu s$



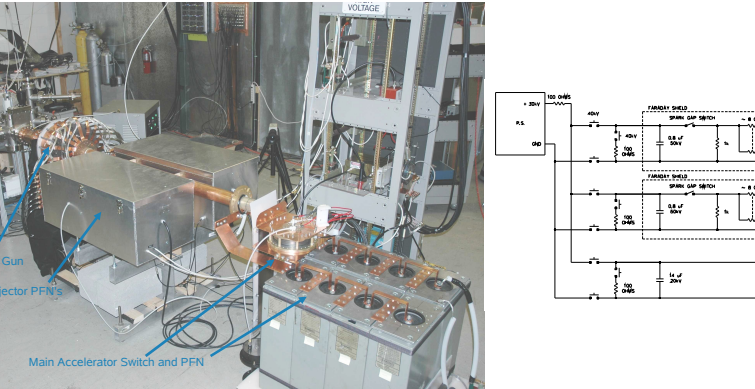
Cross-section of shaped main electrodes with 32 capillary discharge injectors.

Jitter is well in hand - less than 25 ns at 35 kV



[illegible]

HyperV Plasma Jet Accelerator System



The photograph shows the HyperV Plasma Jet Accelerator System. On the left is a large, cylindrical vacuum tank. In the center is the plasma gun, which is connected to the injector PFN's (Pulse Forming Network). To the right is the main accelerator switch and PFN unit, which is a large, rectangular metal box with several circular ports on top. A schematic diagram of the electrical circuit is shown on the right side of the image. The diagram illustrates the power supply, switching, and shielding components of the system.

Voltage

Vacuum Tank

Plasma Gun

Injector PFN's

Main Accelerator Switch and PFN

Capillary driver:
 $0.6\mu F$, $35kV$, $R_{ballast} = 0 - 8\Omega$, $5kA$

Coaxial driver:
 $112\mu F$, $18kV$, $R_{ballast} \sim 40m\Omega$, $180kA$

Switch:
Trigatron, $250kA$, $30kV$

Triggering:
Fiber optic, $1 - 4\mu s$ adj. delay

HyperV Technologies

HyperV Plasma Jet Accelerator System

Vacuum Tank

Plasma Gun

Injector PFN's

Main Accelerator Switch and PFN

Schematic Diagram of the HyperV Plasma Jet Accelerator System:

- Input: +35kV, 100 Ohms
- Components: R.S., 40V, 40V, 100 Ohms, 0.8 uF 50V, 1k, SPARK GAP SWITCH, ~ 8 Ohms, COAX DRIVER, 10 CAPILLARIES
- Output: CAPILLARIES

Capillary driver:
0.6 μF , 35kV, $R_{ballast} = 0 - 8 \Omega$, 5 kA

Coaxial driver:
112 μF , 18kV, $R_{ballast} \sim 40 m\Omega$, 180kA

Switch:
Trigatron, 250kA, 30kV

Triggering:
Fiber optic, 1 – 4 μs adj. delay

HyperV Technologies

HyperV Plasma Jet Accelerator System

Vacuum Tank

Plasma Gun

Injector PFN's

Main Accelerator Switch and PFN

Schematic Diagram of the HyperV Plasma Jet Accelerator System:

- Input: +35kV, 100 Ohms
- Components: R.S., 40V, 40V, 100 Ohms, 0.8 uF 50V, 1k, SPARK GAP SWITCH, ~ 8 Ohms, COAX DRIVER, 10 CAPILLARIES.
- Output: CAPILLARIES

Capillary driver:
0.6 μF , 35kV, $R_{ballast} = 0 - 8 \Omega$, 5 kA

Coaxial driver:
112 μF , 18kV, $R_{ballast} \sim 40 m\Omega$, 180kA

Switch:
Trigatron, 250kA, 30kV

Triggering:
Fiber optic, 1 – 4 μs adj. delay

HyperV Technologies

HyperV Plasma Jet Accelerator System

Vacuum Tank

Plasma Gun

Injector PFN's

Main Accelerator Switch and PFN

Schematic Diagram of the HyperV Plasma Jet Accelerator System:

- Input: +35kV, 100 Ohms
- Components: R.S., 40V, 40V, 100 Ohms, 0.8 uF 50V, 1k, SPARK GAP SWITCH, ~ 8 Ohms, COAX DRIVER, 10 CAPILLARIES
- Output: CAPILLARIES

Capillary driver:
0.6 μF , 35kV, $R_{ballast} = 0 - 8 \Omega$, 5 kA

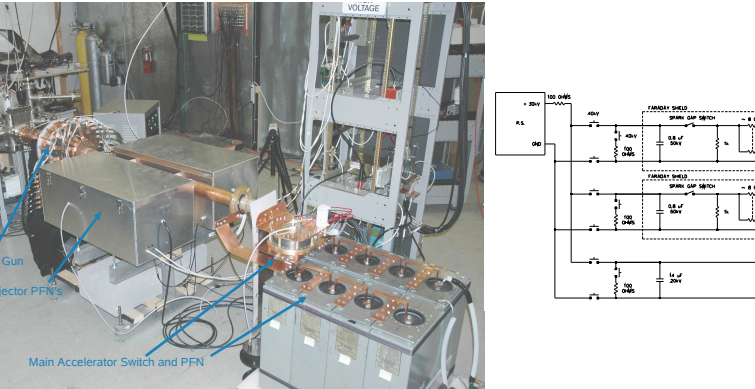
Coaxial driver:
112 μF , 18kV, $R_{ballast} \sim 40 m\Omega$, 180kA

Switch:
Trigatron, 250kA, 30kV

Triggering:
Fiber optic, 1 – 4 μs adj. delay

HyperV Technologies

HyperV Plasma Jet Accelerator System



The photograph shows the HyperV Plasma Jet Accelerator System. On the left is a large, cylindrical vacuum tank. In the center is the plasma gun, which is connected to the injector PFN's (Pulse Forming Network). To the right is the main accelerator switch and PFN unit, which is a large, rectangular metal box with several circular ports on top. A schematic diagram of the electrical circuit is shown on the right side of the image. The diagram illustrates the power supply, switching, and shielding components of the system.

Voltage

Vacuum Tank

Plasma Gun

Injector PFN's

Main Accelerator Switch and PFN

Capillary driver:
 $0.6\mu F$, $35kV$, $R_{ballast} = 0 - 8\Omega$, $5kA$

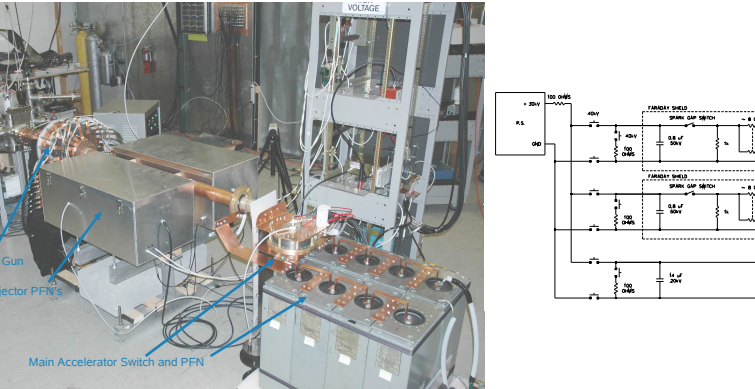
Coaxial driver:
 $112\mu F$, $18kV$, $R_{ballast} \sim 40m\Omega$, $180kA$

Switch:
Trigatron, $250kA$, $30kV$

Triggering:
Fiber optic, $1 - 4\mu s$ adj. delay

HyperV Technologies

HyperV Plasma Jet Accelerator System



The photograph shows the HyperV Plasma Jet Accelerator System. On the left is a large, cylindrical vacuum tank. In the center is the plasma gun, which is connected to the injector PFN's (Pulse Forming Network). To the right is the main accelerator switch and PFN unit, which is a large, rectangular metal box with several circular ports on top. A schematic diagram of the electrical circuit is shown on the right side of the image. The diagram illustrates the power supply, switching, and shielding components of the system.

Voltage

Vacuum Tank

Plasma Gun

Injector PFN's

Main Accelerator Switch and PFN

Capillary driver:
 $0.6\mu F$, $35kV$, $R_{ballast} = 0 - 8\Omega$, $5kA$

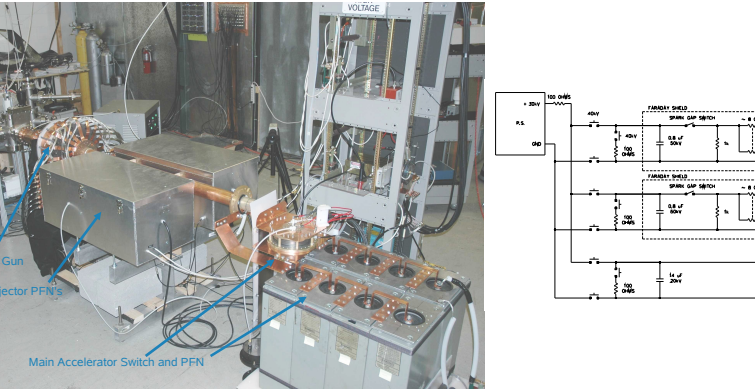
Coaxial driver:
 $112\mu F$, $18kV$, $R_{ballast} \sim 40m\Omega$, $180kA$

Switch:
Trigatron, $250kA$, $30kV$

Triggering:
Fiber optic, $1 - 4\mu s$ adj. delay

HyperV Technologies

HyperV Plasma Jet Accelerator System



The photograph shows the HyperV Plasma Jet Accelerator System. On the left is a large, cylindrical vacuum tank. In the center is the plasma gun, which is connected to the injector PFN's (Pulse Forming Network). To the right is the main accelerator switch and PFN unit, which is a large, rectangular metal box with several circular ports on top. A schematic diagram of the electrical circuit is shown on the right side of the image. The diagram illustrates the power supply, switching, and shielding components of the system.

Voltage

Vacuum Tank

Plasma Gun

Injector PFN's

Main Accelerator Switch and PFN

Capillary driver:
 $0.6\mu F$, $35kV$, $R_{ballast} = 0 - 8\Omega$, $5kA$

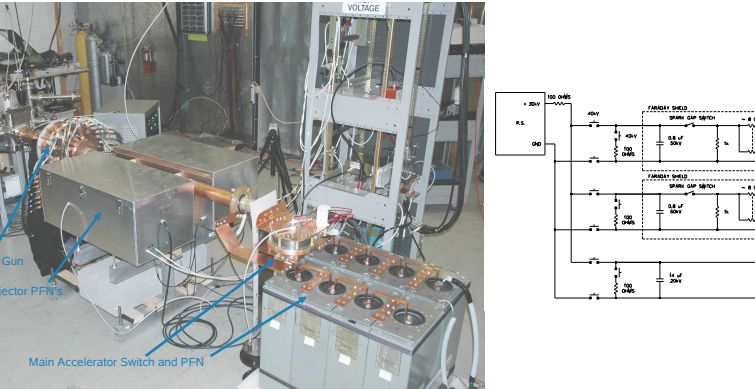
Coaxial driver:
 $112\mu F$, $18kV$, $R_{ballast} \sim 40m\Omega$, $180kA$

Switch:
Trigatron, $250kA$, $30kV$

Triggering:
Fiber optic, $1 - 4\mu s$ adj. delay

HyperV Technologies

HyperV Plasma Jet Accelerator System



The photograph shows the HyperV Plasma Jet Accelerator System. On the left is a large, cylindrical vacuum tank. In the center is the plasma gun, which is connected to the injector PFN's (Pulse Forming Network). The main accelerator switch and PFN unit is located on the right, featuring several large capacitors and a central switch mechanism. Blue arrows point to the vacuum tank, plasma gun, injector PFN's, and the main accelerator switch and PFN unit.

Vacuum Tank
Plasma Gun
Injector PFN's
Main Accelerator Switch and PFN

The schematic diagram on the right illustrates the electrical circuit. It shows a 35kV source connected to a 100 ohm resistor. The circuit is divided into three main sections: the capillary driver, the switch, and the main accelerator. The capillary driver section includes a 40V source, a 40V resistor, a 100 ohm resistor, and a 10 pF capacitor. The switch section includes a 40V source, a 40V resistor, a 100 ohm resistor, and a 10 pF capacitor. The main accelerator section includes a 40V source, a 40V resistor, a 100 ohm resistor, and a 10 pF capacitor. The diagram also shows the Faraday shield, spark gap switch, and coaxial cable connections.

Capillary driver:
 $0.6\mu F$, $35kV$, $R_{ballast} = 0 - 8\ \Omega$, $5\ kA$

Coaxial driver:
 $112\mu F$, $18kV$, $R_{ballast} \sim 40\ m\Omega$, $180kA$

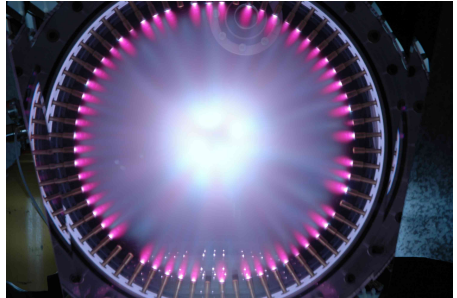
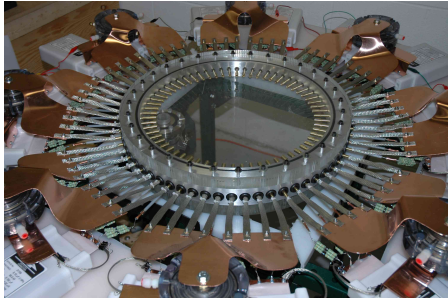
Switch:
Trigatron, $250kA$, $30kV$

Triggering:
Fiber optic, $1 - 4\ \mu s$ adj. delay

HyperV Technologies

The TwoPi Injector Test Fixture

Injector Development and Jet Merging Expts

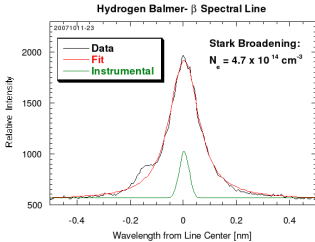


- 64 capillary jets
- 24 inch diameter
- 2 inch vertical gap
- Base pressure 6×10^{-4} Torr

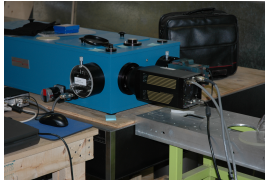
- Brass nozzles
- Tungsten center electrode
- $0.15 \mu F$ Maxwell cap per 4 capillaries at 35 kV
- $R_{ballast} = 1.3 \Omega$

Density and Velocity Spectra

Hydrogen Balmer- β spectrum

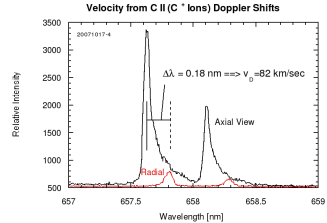


- n_e increases as $R_{ballast}$ decreases
- H_β and H_γ stark broadening are in close agreement
- Stark broadening tends to overestimate density slightly due to radial expansion



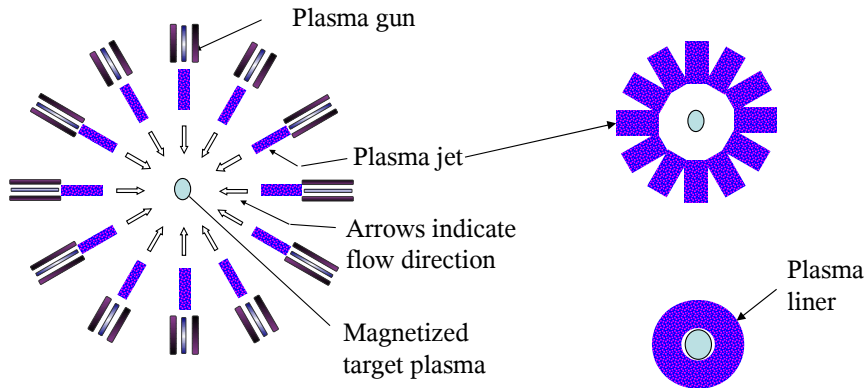
- 1.0 meter focal length f/8 high resolution monochromator
- PI max camera detector

Carbon II spectra



- simultaneous axial and radial views
- H_α shifts \Rightarrow 75 km/s
- Carbon II \Rightarrow 82 km/s
- Carbon III \Rightarrow 71 km/s with significant stationary component
- Carbon IV \Rightarrow 63 km/s no detectable stationary component
- Photodiodes provide cross-check

Merging of High Mach Number Plasma Jets to Form Dense Imploding Plasma Liners¹



An approximately spherical distribution of plasma jets are launched towards a common center.

The jets merge to form a spherical shell (liner), imploding towards the center.

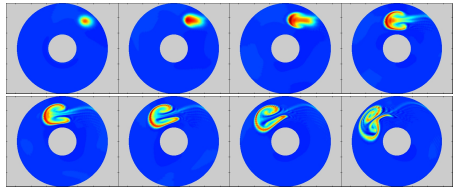
¹Slide courtesy of F. Thio

Use Plasma Jet to Inject Momentum and Drive Rotation in the Maryland Centrifugal eXperiment (MCX)

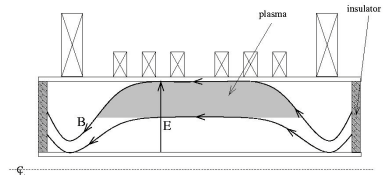
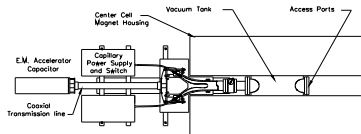
Plasma Gun Mounted on MCX



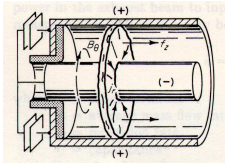
Simulation*



*Courtesy of I. Shamim, A. B. Hassam, and R. F. Ellis - University of Maryland.



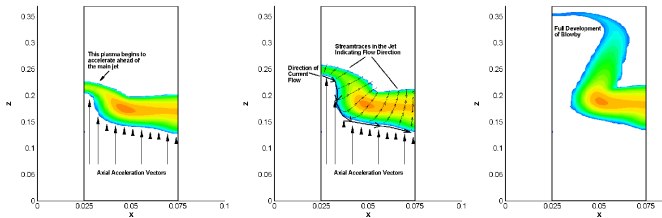
The Blowby Instability Limits Performance of a Classical Straight Coaxial Accelerator



*From R.G. Jahn, "Physics of Electric Propulsion," 1st ed., New York, McGraw-Hill, 1968.

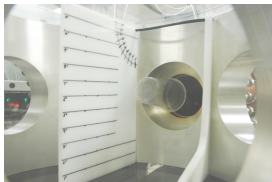
- $B \sim 1/r$
- higher $\vec{j} \times \vec{B}$ near inner electrode
- current distribution is unstable
- $J(r, z)$ "runs away" leaving most mass behind
- must peak density profile near inner electrode

Mass density contour plots illustrate the blow-by instability in a straight coaxial accelerator.*



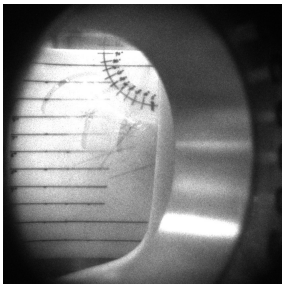
* From J. Cassibry's PhD Dissertation

Ballistic Pendulum Tests

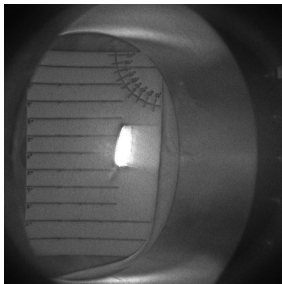


Ballistic Pendulum

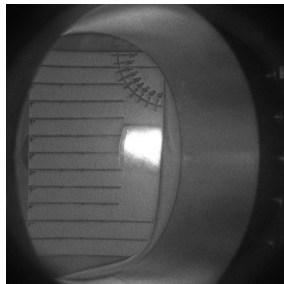
- Pendulum mass = 12.75 gm
- Recoil velocity $\simeq 0.86$ m/s
- Plasma velocity from Doppler shift $\simeq 70$ km/s
- Calculated plasma mass $\simeq 157 \mu\text{g}$
- 11.4 g-m/s



Five $8 \mu\text{s}$ exposures, 100 ms apart, 25 ms delay.



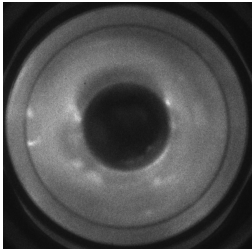
Stagnation on bottom inside of cup. 50 ns exposure at $18.5 \mu\text{s}$.



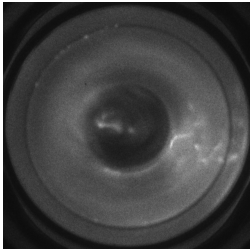
Expansion back to right after impact at $28.5 \mu\text{s}$.

Imaging of Bore Reveals Complex Behavior

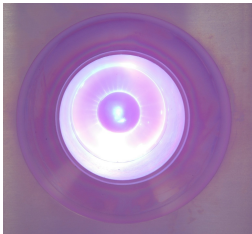
Diffuse plasma structure



Plasma current envelopes tip



Plmax 25 ns images reveal diffuse structure during main current discharge during earlier tests.



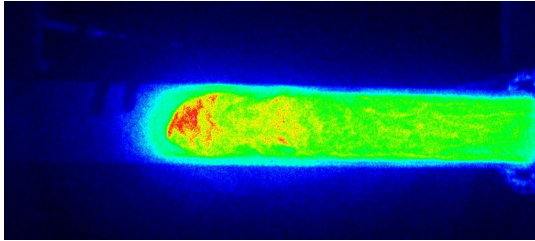
Current pinched on tip



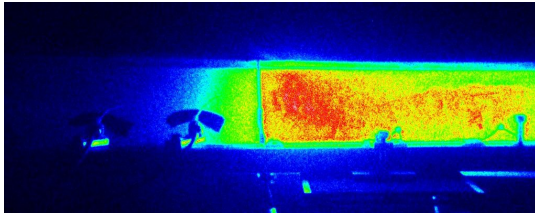
Current fills only left half (contrast enhanced)

2 sec exposures with Nikon D70s (f/29) on recent tests indicate an asymmetry.

Inductive Damping Observed



Plasma slug travels down 1 m long by 10 cm diameter acrylic tube. Visible plasma front is diffuse and bullet shaped.



Passing through one turn of awg14 wire slows, flattens, and compresses the luminous front

False color images from PImax camera. Lower image also shows photodiodes used to view luminous front. Many other conducting rings have been tested with similar results. No velocity damping is observed if conducting loop is broken.